

Utilize Titanium Coating to Increase AZ31 Alloy Corrosion Resistance for Bio-Application**Noor Najm^a, Ali H. Ataiwi^b, and Rana A. Anaee^c**^a University of Thi – Qar- Petroleum & Gas Eng. Department, Iraq^b Ashur University College, Iraq^c University of Technology – Materials Eng. Department, Iraq

*Corresponding author: noornajm@utq.edu.iq

Abstract

The behavior of corrosion of AZ31 Mg alloy was studied in (SBF) “Simulated Body Fluid” by electrochemical analysis technique to realize the role of coating with (Ti) by DC sputtering with the absence and presence of oxygen. The coating by (Ti) with the absence of oxygen enhanced the stability of the corrosion product as MgO through decreasing the corrosion current density. While the presence of oxygen during coating accelerated the corrosion rate due to increasing the cathodic polarization through the reduction of oxygen and then increasing the dissolution of Mg from the substrate. The coating by (Ti) gave protection efficiency reach (33.742%). While the presence of oxygen during DC sputtering promotes the cathodic area on grains as (TiO₂) leading to localizing the corrosion around the *AlMn* phases at the grain boundaries.

Keywords: AZ 31 Mg alloy, Biodegradability, SBF, DC Sputtering, Titanium Coating, Electrochemical Analysis.

1. Introduction

A new promising materials classes are Magnesium alloys, currently under development [1], and it shows weak resistance to corrosion in physiologic environments containing Cl⁻. Therefore, the alloy of these metals can be utilized as a biodegradable implant. Furthermore, Magnesium is an essential component of human metabolism and one of the body's most abundant cations, as it comes in the fourth sequence [2]. In addition, the biodegradation rate of these alloys is usually quite high. Often this degradation happens in the beginning of the implantation stage [3,4]. In biomedical implants, it is considered the limitations of its utilization. The high degradation rate of Mg presents a number of troubles: A. During the degradation of metal, it produced subcutaneous bubbles of hydrogen which can cause hydrogen accumulation about the implant. It can influence the operation of healing, in addition to causing tissue necrosis via means of formation of gaps between the tissue and the implant [3,5,6].

B. Through the cathodic reaction of the corrosion operation occurs alter in local pH magnitudes caused by the creation of OH⁻ anions [7]. This operation affects several cell viability and cellular functions [3]. C. The significant corrosion rate of magnesium

causes early degeneration of the implants' transverse sections. [8]. Several writers have claimed in earlier studies that the time it takes for magnesium to degrade is shorter than the time it takes to acquire mechanical integrity. [9]. However, many factors affect the implant stability period, such is the study kind (in vitro and in vivo), material composition, implant site, type of model (various animals), and in-vivo test evaluation days. Although there are many ways to measure degradation rates, correlations with in vitro testing are not easy to obtain. Therefore, improving the surface properties of magnesium and related alloys has become critical in order to improve corrosion resistance and biocompatibility while maintaining bulk material qualities [10]. For the use of magnesium and its alloys in absorbable implants as new biomaterials, attention must be paid to developing their corrosion rate because it is a major factor. As a result, coatings have been used as a possible method to reduce degradation in the early stages of the cultured materials and have a good effect on the tissue restoration process. The surface of magnesium can be modified to prevent electrolytes in biological medium or electrolyte solutions from rapidly degrading the material [11,12].

Hanas et al. (2016) used AZ31 magnesium alloy pre-treated by electrospinning with nitric acid and study the effect coating of a PCL/nHA composite. The extracellular morphology of electrospun fibrous

PCL/nHA coating worked as a stable scaffold for rapid biomineralization, according to the tests. During the immersion test, the uncoated samples degraded at a pace that was more than half that of the

covered samples. In addition, It resulted in a significant increase in percentage cell viability of more than 50%. Furthermore, despite the cells flattening and expanding on the composite coated sample due to the distinctive coating morphology, the uncoated sample demonstrated poor cell adherence with super cytocompatibility [13]. Perumal et al. (2020) The in vivo behavior of New Zealand white rabbits was tested using a dip-coating approach followed by electrospinning for the AZ31 cage implant, where the coating material was a bilayer of PCL/nHA. The outcomes revealed improved

The important goal of paper is to develop a biodegradability implant of AZ31 Mg alloy by coating with titanium using DC sputtering technique with and without oxygen.

2. Experimental Procedure

2.1 Materials and methods

The chemical compositions for commercial as cast AZ31 alloy ingots in table 1 which obtained from Iraq's Ministry of Industry and Minerals (AMETEK, SPECTRO MAXx). Firstly, samples with dimensions of (2 × 15 × 20 mm) are cut from the as-cast AZ31 plate by CNC water jet machining, then they are mechanically polished and immersed in ethanol for five minutes.

Under argon vacuum furnace atmosphere protection, the samples were prepared by annealing for 90 minutes at the temperature of 350°C, still in a furnace until room temperature, with an accuracy of ±1°C. Finally, samples were a magnetron sputtering 1500 system was used to deposit Ti-doped thin films on AZ31 substrates. Ti (99.992%) targets with a 5-inch diameter were used to create the coatings.

Table 1 . Chemical compositions for commercial as cast AZ31 alloy

Metal	Si	Zn	Ca	Cu	Mn	Fe	Ni	Al	Mg
Wt%	0.0014	1.361	0.180	0.004	0.291	0.003	0.002	3.623	Rem.

2.2. Characterizations

Kashan University in Iran has an X-ray diffraction type (Dandong Haoyuan DX-2700B, X-ray Diffractometer) with the following specifications: X-ray tube: Cu, NF (1.54060 nm), scanning radius: 185 mm, X-ray leakage: less than 2.5Sv/h when used to create phases. Scanning electron microscope

controlled biodegradation of the implant and healing of bone at the diseased site [14]. Nikbakht et al. (2021) Studied the effect of pre-treatment with hydraulic acid for AZ31 alloy followed by HA - dispersion silane coating. The results showed improved cell proliferation and enhanced resistance to degradation up to three orders of magnitude when using HA nanoparticles (size >200 nm) dispersed in a silane coating, while higher HA dispersion in the silane solution beyond 1,000 mg/L resulted in rapid deterioration due to particle aggregation [15].

(SEM) at Tehran University in Iran was used to study the microstructure.

2.3. Electrochemical corrosion Analysis

To measure the dynamic effective polarization curves, a device that is controlled by a computer (Warminster, PCI4/750, PA, GAMRY, Inc.) and an SBF solution were used at a human body temperature of (37°C). A noble metal (platinum) is used as a counter electrode and Ag/AgCl as a reference electrode while a specimen holder is used for AZ31 specimens as a working electrode with (1 cm²) territory that is exposed. A constant open circuit potential ((E_{OCP}) was registered during the first 90 minutes after dipping into the solution [16].

3. Discussion of the Findings

3.1. Analysis of X-Ray Diffraction

The XRD models of annealed AZ31 alloy before and after coating appear in Figure 1, identifying the different phases made up of α-Mg and the second phase as -Mg₁₇Al₁₂. Gajanan et al., who researched the behavior of corrosion and mechanical properties following grain refinement by equal channel angular extrusion for Mg alloy, also identified these phases. [17]. According to “JCPDS” card No. 35-0821, the primary peak of α -Mg appears at 2 equal to 36.619. The primary peak at 2 equal to 32.541, 38.481, and 59.605 can be seen in the XRD pattern of Ti coating on Mg alloy, which was created using a DC sputtering technology to deposit a thin film of elements in the target (according to “JCPDS” card No. 44-1288). The presence of oxygen within the DC sputtering process leads to producing metal oxides as (TiO₂) with 2θ values of 33.575 and 34.098 (according to “JCPDS” card No. 33-1381).

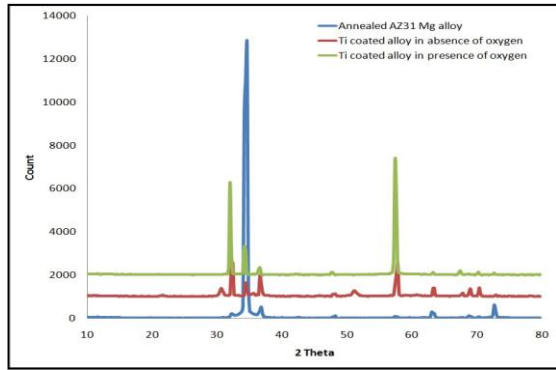


Fig. 1. XRD patterns of annealed AZ31 alloy before and after coating.

3.2. Microstructural Examination

The evolution of the microstructure of AZ31 induced by the annealing treatment is shown in Figure (2). It contains a mixture of fine and coarse balanced. It consists of a white phase by (α -Mg) surrounded by an intermetallic compound dark phase represented by ($Mg_{17}Al_{12}$) particles. At the grain boundaries and in the overlapping regions there are various forms of precipitated $Mg_{17}Al_{12}$. The use of an annealing heat treatment at 350°C for 90 minutes was shown to be successful in dissolving the ($Mg_{17}Al_{12}$) precipitate in the cast ingot and lowering the $Mg_{17}Al_{12}$ area percentage [18,19]. In addition, there are points, lamellar and island-like second phases ($Mg_{17}Al_{12}$) surrounding the island-like phase as seen in Figure (2). The precipitate point-like undergoes re-dissolving in the matrix after annealing treatment, then a large number of β - $Mg_{17}Al_{12}$ second lamellar phase precipitates at or near the grain boundaries and diffuses into the grains [20, 21].

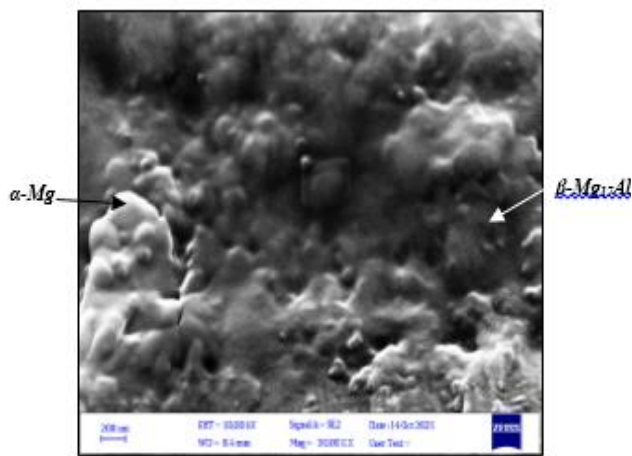
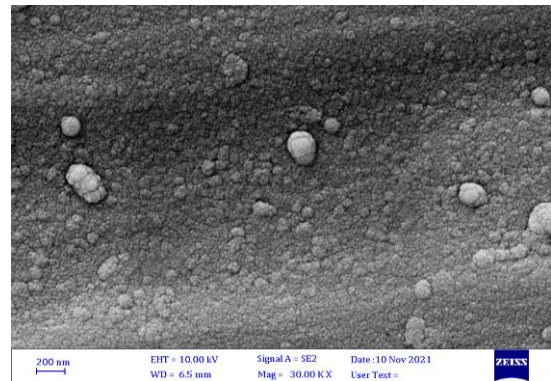


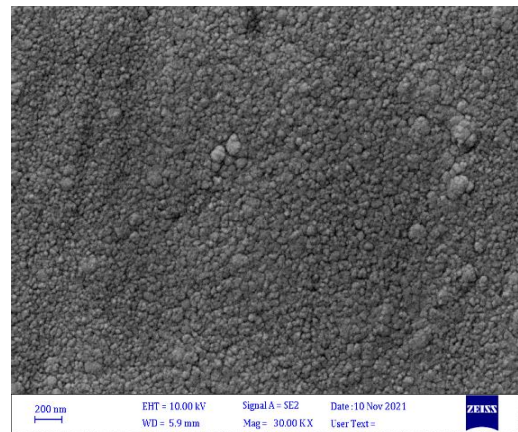
Fig. 2. SEM of annealed AZ31 Mg alloy.

The SEM photos of samples coated with (Ti) without and with oxygen are illustrated in Figure (3).

The SEM image of Ti coated AZ31 Mg alloy shows a highly homogeneous surface with a compact uniform layer, which could be attributable to the creation of a stable titanium layer, while the deposition of Ti with oxygen gives a macroscopically flat surface but slightly rough (Fig. 3-b) which agrees with the deposition of TiO_2 on MgZn alloy by magnetron sputtering [22].



(a)

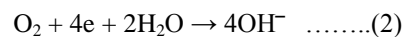
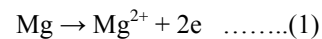


(b)

Fig.3. SEM of coated AZ31 alloy by (a) Ti, and (b) Ti+O.

3.3. Corrosion Measurement

The corrosion of Mg alloys can occur in some phases and these secondary phases may protect material or accelerate the corrosion rate by forming stable areas or galvanic cells respectively according to interaction with the corrosive environment. The result is forming magnesium hydroxide $Mg(OH)_2$ and magnesium oxide (MgO) is an unstable passive film after anodic and cathodic reactions as shown below:



Generally, the role of coating is to produce a barrier to prevent the connection between the materials and corrosive medium. The coating by *Ti* element in the absence and presence of oxygen was applied on AZ31 Mg alloy, which was done by using DC sputtering, to investigate the corrosion properties of Ti coated specimens.

The open circuit potential (E_{oc}) is estimated from potential–time measurement for immersion time of (3600 sec) for bioapplication. Fig. (5 a) shows this behavior which gives variation in (E_{oc}) value which may be shifted to the active or positive direction. This behavior interprets the nature of magnesium oxide on the surface that is incorporated with the coating layer. It is clear from Tafel plots for uncoated and coated specimens that the coating by titanium metal without oxygen may little reduce corrosion (i.e., reduces corrosion current density i_{corr}) and shift the corrosion potential (E_{corr}) to noble direction, while the coating in presence of oxygen gives negative effect and increases corrosion and shift (E_{corr}) to cathodic direction due to their act as cathodic areas. The formation of ($MgAl_2O_4$) and magnesium hydroxide on AZ 31 Mg alloy surface [23] may interact with coating components to enhance the galvanic cells for corrosion and the acceleration can occur. Also, the pits may be initiated around the *AlMn* phases and located at the grain boundary [24] or the grain boundaries may produce a barrier to retard the initiation of corrosion [25, 26] with different mechanisms that refer to poor resistance in (SBF) for Mg alloy [27].

The inverse effect of titanium coating in the presence of oxygen comes from the nature of oxide layers that formed on grains and accelerate the corrosion at grain boundaries where (TiO_2) may act as a cathodic area leading to localized corrosion on Mg base alloy.

Little efficiencies have been obtained for coating by (Ti) equal to (33.742%) that calculated according to the following formula [28]:

$$PE\% = \left[1 - \frac{i_{corr,coated}}{i_{corr,uncoated}} \right] \times 100 \dots\dots(3)$$

where; (PE%) is protection efficiency, ($i_{corr, coated}$) and ($i_{corr, uncoated}$) are the after and before-coating corrosion current densities, respectively.

When polarization resistance (R_p) is computed using Tafel slopes and corrosion current density, it can be observed that the resistance was reduced after titanium coating, as estimated using the Stern-Geary equation [29]:

$$R_p = \frac{b_a \times b_c}{2.3 i_{corr}(b_a + b_c)} \dots\dots(4)$$

The anodic and cathodic slopes of Tafel in mV.dec-1 are (b_a and b_c).

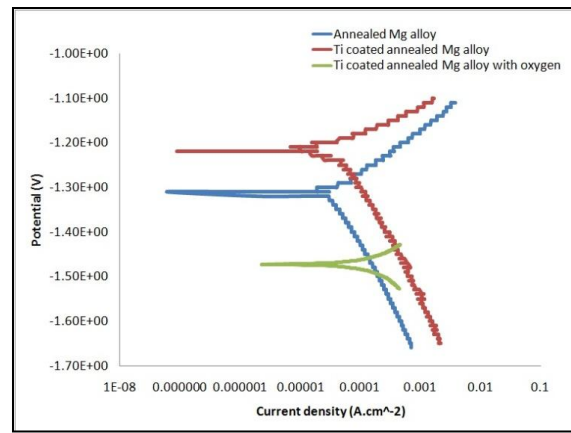
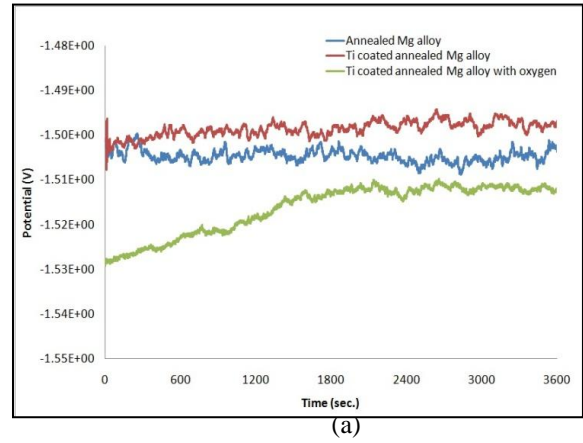


Fig. 4. Electrochemical properties of treated AZ 31 Mg alloy as (a) OCP and (b) Tafel plot.

Table 2. Data of Corrosion AZ31 Mg alloy annealed and coated in SBF at 37°C.

Sample	- E_{corr} (V)	$i_{corr} \times 10^{-5}$ (A.cm ⁻²)	- b_c (mV.dec ⁻¹)	+ b_a (mV.dec ⁻¹)	C_R (mpy)	PE (%)	$R_p \times 10^2$ (Ω.cm ²)
Annealed alloy	1.3149	5.2584	110.63	339.11	0.478	-	6.897
Coated with Ti	1.2187	3.4841	69.98	196.50	0.317	33.742	6.440
Coated with Ti+O	1.4730	64.787	243.28	465.17	5.889	-	1.072

Conclusion

The AZ31 magnesium alloy was annealed and coated with titanium with and without oxygen using the DC magnetron sputtering technique to minimize its corrosion rate. The results are:

- 1- The coated titanium with absence oxygen showed that the protection efficiency was equal to (33.742 %) and the corrosion rate decreased from 0.478 (mpy) to 0.317 (mpy).
- 2- The coated titanium with the presence of oxygen leads to get bad efficiency due to the formation of titanium oxide before the incorporation of titanium with elements of Mg alloy.
- 3- These results have been supported by XRD analysis, SEM exam, and electrochemical analysis.

References

- [1] Farraro, K., Kim, K., Woo, S., Flowers, J. and McCullough, M. "Revolutionizing orthopaedic biomaterials: The potential of biodegradable and bioresorbable magnesium-based materials for functional tissue engineering", *J. Biomechanics*, vol. 47,9, 2014.
- [2] Gu, X. and Zheng, Y., "A review on magnesium alloys as biodegradable materials", *Frontiers of Materials Science in China*, 2010, 4,111.
- [3] Witecka, A., Bogucka, A., Yamamoto, A., Máthis, K., Krajnák, T., Jaroszewicz, J. and Swieszkowski, W., "In vitro degradation of ZM21 magnesium alloy in simulated body fluids", *J. Materials Science and Engineering C*, 65, 2016, 59.
- [4] Poinern, E., Brundavanam, S. and Fawcett, D., "Biomedical magnesium alloys: A review of material properties, surface modifications and potential as a biodegradable orthopaedic implant", *American Journal of Biomedical Engineering*, 2, 2013, 218.
- [5] Song G., "Control of biodegradation of biocompatible magnesium alloys", *Corrosion Science*, 49, 2007,1696.
- [6] Peng, W., Tan, L. and Yang, K., "Surface modification on biodegradable magnesium alloys as orthopedic implant materials to improve the bio-adaptability: A review", *J. Materials Science & Technology*, 32, 2016,827.
- [7] Hornberger, H., Virtanen, S. and Boccaccini, A., "Biomedical coatings on magnesium alloys – A review", *Acta Biomaterialia*, 8, 2012, 244.
- [8] Agarwal, S., Curtin, J., Duffy, B. and Jaiswal, S., "Biodegradable magnesium alloys for orthopaedic applications: A review on corrosion, biocompatibility and surface modifications", *J. Materials Science and Engineering* 90, 2016,15.
- [9] Zheng, Y., Gu, X.N. and Witte, F., "Biodegradable metals", *J. Materials Science and Engineering: R: Reports*, 77, 2014,1.
- [10] Sanchez, A., Luthringer, B., Feyerabend, F. and Willumeit, R., "Mg and Mg Alloys: How comparable are in vitro and in vivo corrosion rates? A review", *Acta Biomaterialia*. 13, 2015, 16.
- [11] Peltola, T., Patsi, M. Rahiala, H., Kangasniemi, I. and Yli-Urpo, A., "Calcium phosphate induction by sol-gel-derived titania coatings on titanium substrates in vitro", *J. Biomedical Materials Research*, 41, 1998,504.
- [12] Burnat, B., Robak, J., Batory, D., Leniart, A., Piwonski, I., Skrzypek, S. and Brycht, M., "Surface characterization, corrosion properties and bioactivity of Ca-Doped TiO₂ coatings for biomedical applications", *Surface and Coatings Technology*, 280, 2015, 291.
- [13] Hanas, T., Sampath Kumar, T. S., Perumal, G., and Doble, M. "Tailoring Degradation of AZ31 alloy by Surface Pre-treatment and Electrospun PCL Fibrous Coating", *Mater. Sci. Eng.*, 65, 2016, 43.
- [14] Peral, L. B., Zafra, A., Bagherifard, S., Guagliano, M., and Fernández-Pariente, I. "Effect of Warm Shot Peening Treatments on Surface Properties and Corrosion Behavior of AZ31 Magnesium alloy", *Surf. Coat. Tech.* 401, 2020, 126285.
- [15] Nikbakht, A., Dehghanian, C., and Parichehr, R. "Silane Coatings Modified with Hydroxyapatite Nanoparticles to Enhance the Biocompatibility and Corrosion Resistance of a Magnesium alloy", *RSC Adv.* 11, 2021, 26127.
- [16] Rana Afif Anae, Abdullah A. Abdulkarim, Mathew T. Mathew, Hiyam Mezher Jedy, "The Effect of Nb₂O₅-Ni Coatings on the Microstructural and Corrosion Behavior on Carbon Steel for Marine Application", *J. Bio- and Tribo-Corrosion* ,7, 2021,1.

- [17] M N Gajanan, S Narendranath and S S Sathesh Kumar, "Effect of grain refinement on mechanical and corrosion behavior of AZ91 magnesium alloy processed by ECAE", *J. Materials Science and Engineering*, 591, 2019,012.
- [18] A. Kandil, "Microstructure and mechanical properties of Sicp/Az91 magnesium matrix composites processed by stir casting," *J. JES. Eng.*, 40, 2012, 255.
- [19] Y. Zhang, M. Li, W. L. Yang, Z. G. Wang, and X. Z. Wang, "Microstructural evolution and mechanical properties of as-cast Mg-12Zn alloys with different al additions," *Mater. Res.*,23, 2020,1.
- [20] Z. Yang, "Multimodal microstructure and mechanical properties of AZ91 Mg alloy prepared by equal channel angular pressing plus aging," *Metals (Basel)*, 2018.
- [21] A. Chu, Y. Zhao, R. Ud-Din, H. Hu, Q. Zhi, and Z. Wang, "Microstructure and properties of Mg-Al-Ca-Mn alloy with high Ca/Al ratio fabricated by hot extrusion," *Materials (Basel)*, 14, 2021,1.
- [22] Shusen Hou, Weixin, Zhijun Yang, Yue Li, Lin Yang, and Shaoting Lang, "Properties of Titanium Oxide Coating on MgZn Alloy by Magnetron Sputtering for Stent Application", *Coatings*, 2020,10, 999.
- [23] Fumin Xu, Lan Luo, Yong Liu, JunWan and Guixing Xu, "Microstructure and corrosion behaviors of AZ31 alloy with an amorphous-crystallin nano-composite film", *Mater. Res. Express* (2020), IOP Publishing.
- [24] Song GL, Xu Z. "The surface, microstructure and corrosion of magnesium alloy AZ31 sheet", *Electrochim Acta* , 2010,55.
- [25] Argade GR, Panigrahi SK, Mishra RS. "Effects of grain size on the corrosion resistance of wrought magnesium alloys containing neodymium", *Corrosion Sci*, 2012, 58.
- [26] Pawar S, Slater TJA, Burnett TL, Zhou X, Scamans GM, Fan Z, et al. "Crystallographic effects on the corrosion of twin roll cast AZ31 Mg alloy sheet", *Acta Mater* 2017,133.
- [27] Rupesh Chalishgaonkar, "Insight in applications, manufacturing and corrosion behavior of magnesium and its alloys – A review", *J. Materials today Proceeding*, 26, 2020, 1060.
- [28] T.A. Alkarim, K.F. Al-Azawi and R.A. Anaee, "Anticorrosive properties of Spiramycin for aluminum in acidic medium", *Int. J. Corros. Scale Inhib* 10, 2021, 1168 .
- [29] Rana A. Anaee, Ivan H. Tomi, Majid H. Abdulmajeed, Shaimaa A. Naser, and Mustafa M. Kathem, "Expired Etoricoxib as a corrosion inhibitor for steel in acidic solution", *J. Molecular Liquids* 279, 2019, 549.